Bias voltage control of magnetic phase transitions in graphene nanojunctions

2015 Nanotechnology 26 345203

(http://iopscience.iop.org/0957-4484/26/34/345203)

IOP Publishing Nanotechnology
Nanotechnology 26 (2015) 345203 (5pp) doi:10.1088/0957-4484/26/34/345203

Bias voltage control of magnetic phase transitions in graphene nanojunctions

Kaikai Luo[1] **and Weidong Sheng**[2]

[1] State Key Laboratory of Surface Physics and Department of Physics, Fudan University, Shanghai 200433, People's Republic of China
[2] State Key Laboratory of Surface Physics, Collaborative Innovation Center of Advanced Microstructures, and Department of Physics, Fudan University, Shanghai 200433, People's Republic of China

E-mail: shengw@fudan.edu.cn

Received 13 April 2015, revised 1 July 2015
Accepted for publication 13 July 2015
Published 5 August 2015

Abstract

The magnetic state of a spintronic device is usually controlled by magnetic contacts or a transverse electric field generated by side gates. In this work, we consider a graphene nanojunction in the presence of a bias voltage that leads to magnetic phase transitions in the system. Combining the non-equilibrium Green's function with the Hubbard model, our self-consistent calculation reveals that an increasing bias voltage induces consecutive transitions among antiferromagnetic and ferromagnetic states. It is further shown that the graphene nanojunction is turned off in the antiferromagnetic state when the bias voltage is low and can then be switched on to the ferromagnetic state by a high bias voltage. We therefore demonstrate that the magnetic state of the graphene system can be controlled by the bias voltage without resorting to any transverse gates.

Keywords: bias voltage, magnetic phase transition, graphene nanojunction

(Some figures may appear in colour only in the online journal)

1. Introduction

Due to its unique and superior electronic and magnetic properties [1], graphene [2] has been regarded as a potential candidate for future spintronic devices [3–7]. Since a finite zigzag graphene nanoribbon is shown to have a ground state with spin polarized along its edges [8], various methods have been proposed for manipulation of its magnetism such as hydrogenation [9], the photonic method [10], and the application of external magnetic [11] or electric [12–14] field. Meanwhile, spin-polarized transport in graphene has become an interesting issue and a number of different functional devices like the field-effect transistor [15, 16], spin valve [17, 18], spin filter [19], negative differential resistance [20], and giant magnetoresistance [21] have been proposed.

A successful spintronic application relies on the efficient control of the magnetic state of the device, usually by means of an applied electric field. In general, the external electric field is introduced by the gate voltage in a standard field-effect transistor structure. It has already been shown that a zigzag graphene nanoribbon may become a half-metallic material if an in-plane electric field is applied across its zigzag edges [22]. Hence, zigzag ribbon devices are expected to fulfill the functions of a spin filter and spin transistor through transverse electric fields without resorting to any magnetic contacts [23, 24]. However, by doing so, a standard field-effect transistor structure has to be implemented, which increases the complexity of the spintronic device.

An alternative and maybe arguably better way, as proposed in this work, is to make good use of the bias voltage. For electron transport, a bias voltage is essential for providing current through the device. However, it also helps to establish an electric field along the current direction. While being perpendicular to the transverse field induced by the gate voltage, this electric field is expected to play a similar role, such as favoring different magnetic configurations. For a zigzag nanoribbon, a high bias voltage is shown destroy a polarized spin configuration, leading the device into a non-magnetic state [25]. In this work, we show that a bias voltage applied to a graphene nanojunction induces consecutive transitions among its antiferromagnetic (AFM) and ferromagnetic (FM) states. Under low bias voltage, we find that

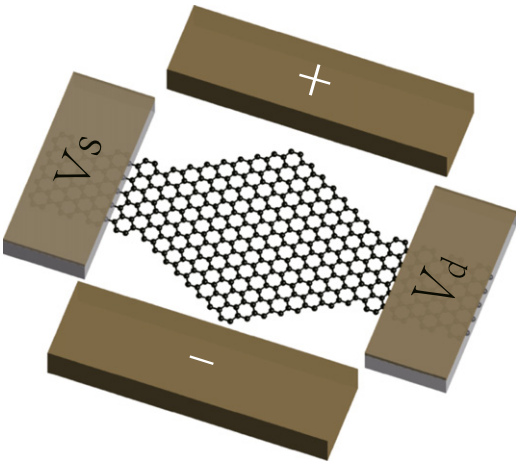

Figure 1. Schematic diagram of a diamond-shaped graphene nanojunction. The source and drain metallic electrodes are labeled by V_s and V_d, respectively. A pair of side gates which generate a transverse electric field are labeled by + and –, respectively.

the device is in a stable antiferromagnetic state which blocks most of the electron transport and therefore effectively sets the device into an OFF state. When the bias voltage increases, we show that the device can be switched on to the ferromagnetic state and allows spin polarized current.

A common approach for the study of electron transport through a molecular system is to combine the non-equilibrium Green's function (NEGF) formalism with density functional theory [26, 27]. For a device with a large number of atoms like the one shown in figure 1, this kind of method requires a great computational resource. For simplicity, a model Hamiltonian like the Hubbard model is usually adopted to obtain the main features of the electron transport through a graphene system. However, the electrostatic profile is often oversimplified to a flat line inside the device, with the bias voltage drop largely occurring at the contacts in various empirical models. In this work, we use the method of moments to obtain a realistic electrostatic potential in the self-consistent calculation.

2. Method and model

Figure 1 depicts our model system, a graphene nanojunction with four zigzag edges. Two semi-infinite electrodes attached to the device are made of metallic armchair graphene ribbons and function as source and drain. For comparison, we also introduce a pair of side gates that generates a transverse electric field. Similar devices have already been realized in the experiments [28, 29].

In the linear transport regime where the bias voltage is small, the system is in equilibrium and thus has a uniform Fermi energy E_F. When the bias voltage becomes large, the system enters into the non-equilibrium regime and the local Fermi level can be written as $u = E_F \pm e(V_s - V_d)/2$ for the left and right electrode, respectively. Here $V_s - V_d$ is the bias voltage. To investigate the effect of bias voltage on the spin-polarized electron transport, we need to first calculate the Green's function of the device within the NEGF formalism. It is given by

$$G_c = \left[E - H - \Sigma_s - \Sigma_d\right]^{-1}, \tag{1}$$

$$\Sigma_s = h_{sc}^{\dagger} \cdot g_s \cdot h_{sc}, \ \Sigma_d = h_{dc} \cdot g_d \cdot h_{dc}^{\dagger}, \tag{2}$$

where Σ_s and Σ_d are the self-energies for the source and drain, respectively, g_s and g_d are the the surface Green's functions, h_{sc} and h_{dc} are the coupling matrices between the device and electrodes. The spin-dependent transmission can then be obtained by [30]

$$T_\sigma(E) = \mathrm{Tr}\left[\Gamma_{\sigma,s}(E) G_{\sigma,c}(E + i\epsilon) \Gamma_{\sigma,d}(E) G_{\sigma,c}(E - i\epsilon)\right], \tag{3}$$

where the broadening function $\Gamma_{\sigma,s(d)}(E)$ is defined by

$$\Gamma_{\sigma,s(d)}(E) = i\left[\Sigma_{\sigma,s(d)}(E) - \Sigma_{\sigma,s(d)}^{\dagger}(E)\right]. \tag{4}$$

This function relates the broadening to the finite lifetime of the electronic states, reflecting the fact that an electron introduced into the state does not stay there forever, but leaks away into the contact. The spin-resolved current is then given by

$$I_\sigma(V_s - V_d) = \frac{e}{h} \int T_\sigma(E)\left[f(E - \mu_s) - f(E - \mu_d)\right] dE, \tag{5}$$

with $f_{s(d)}(E)$ being the Fermi–Dirac distribution function of the source (drain)

$$f_{s(d)}(E) = \left[1 + e^{\left(E - \mu_{s(d)}\right)/k_B T}\right]^{-1}, \tag{6}$$

which is mainly affected by temperature T and chemical potential $\mu_{s(d)} = -eV_{s(d)}$. Hence we have the total current $I = I_\uparrow + I_\downarrow$ and spin-polarized current $I_{sp} = I_\uparrow - I_\downarrow$.

To describe the electronic structure of the graphene nanojunction, we adopt the Hubbard Hamiltonian

$$H = -t \sum_{ij\sigma} \left(c_{i\sigma}^{\dagger} c_{j\sigma} + c_{j\sigma}^{\dagger} c_{i\sigma}\right) + U \sum_i n_{i,\sigma} n_{i,-\sigma} \tag{7}$$

which has been widely used to investigate the magnetic properties of graphene devices [1]. Here $n_{i\sigma} = c_{i\sigma}^{\dagger} c_{i\sigma}$ is the electron density operator for spin σ on site i. Here we choose $t = 2.7$ eV and $U/t = 2.0$. Within the mean-field approximation, the Hubbard term can then be replaced by $(\langle n_{i,\uparrow}\rangle - \frac{1}{2}) n_{i,\downarrow} + (\langle n_{i,\downarrow}\rangle - \frac{1}{2}) n_{i,\uparrow}$.

In the non-linear transport regime, the electron density matrix consists of two parts: the equilibrium part and non-equilibrium part [31]. The former can be calculated by using a contour integral [32] in the complex plane, while the latter can be obtained by integration on the real axis with a rectangular quadrature scheme. Following the calculation of the electron density, the electrostatic potential profile in the nanojunction device [33] can be determined by using the method of moments [34]. By partitioning the system into the device (D) and contact (C) sectors, we can write Poisson's equation in matrix form as follows,

$$\begin{bmatrix} \varphi_D \\ \varphi_C \end{bmatrix} = \begin{bmatrix} U_{DD} & U_{DC} \\ U_{DC} & U_{DC} \end{bmatrix} \begin{bmatrix} n_D \\ n_C \end{bmatrix}. \tag{8}$$

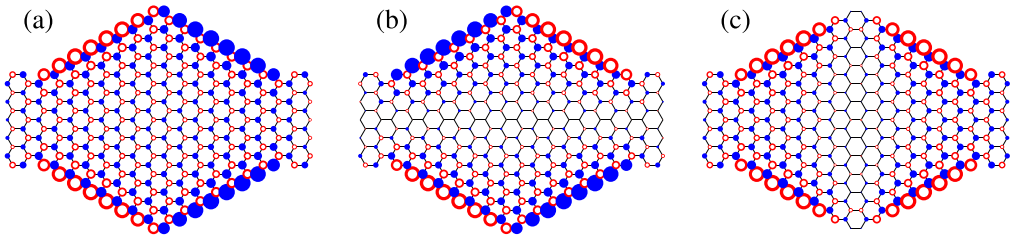

Figure 2. Local spin densities calculated for three stable configurations. (a) and (b) are AFM states while (c) is a FM state. Solid and open dots correspond to different spins.

Here $\phi_{D(C)}$ is the electrostatic potential and $n_{D(C)}$ is the electron density. After some algebra, we rearrange the equations to obtain the potential in the device [35]

$$\phi_D = U_{DC}U_{CC}^{-1}\phi_C + \left(U_{DD} - U_{DC}U_{CC}^{-1}U_{CD}\right)n_D \tag{9}$$

The Coulomb matrix U_{ij} is given by the Pariser–Parr–Pople model within the Matago–Nishimoto approximation [36],

$$U_{ij} = \frac{e^2}{\left|r_i - r_j\right| + \dfrac{2e^2}{U_{ii} + U_{jj}}} \tag{10}$$

Starting from various spin configurations [37], we are able to determine a number of stable spin-polarized states after the self-consistent procedure reaches its convergence. The energies of these states can be obtained by

$$E = \sum_{i,\sigma} e_\sigma^{(eq)}(ii) + e_\sigma^{(neq)}(ii). \tag{11}$$

Here $e_\sigma^{(eq)}$ and $e_\sigma^{(neq)}$ are the equilibrium and non-equilibrium parts of the energy density matrix which can be calculated in a similar way to the density matrix.

3. Result and discussion

Figure 2 depicts three stable spin configurations, two of which are AFM states (AFM1 and AFM2) and the other a FM state, obtained by the self-consistent calculation. In AFM1, the spins have the same polarization near each electrode and the nanojunction and it hence looks like two ferromagnetic parts with opposite magnetization connecting with each other. In contrast, AFM2 is seen to consist of two antiferromagnetic sections together and thus the device is weakly polarized in the middle. In the FM state, the spins have the same polarization along all four zigzag edges.

Figure 3 plots the current as a function of the bias voltage calculated for three different spin configurations. Here we set the temperature $T = 293$ K. First it is found that the current is nearly shut off as the nanojunction is in the AFM1 state. On the contrary, the device is seen to exhibit a linear *I/V* curve, i.e., with an almost constant conductance, when being occupied by the AFM2 state. As for the FM state, it is found that the device is first shut off as the bias voltage is smaller than about 0.15 V, and the current then increases rapidly after the bias voltage reaches 0.2 V and eventually saturates.

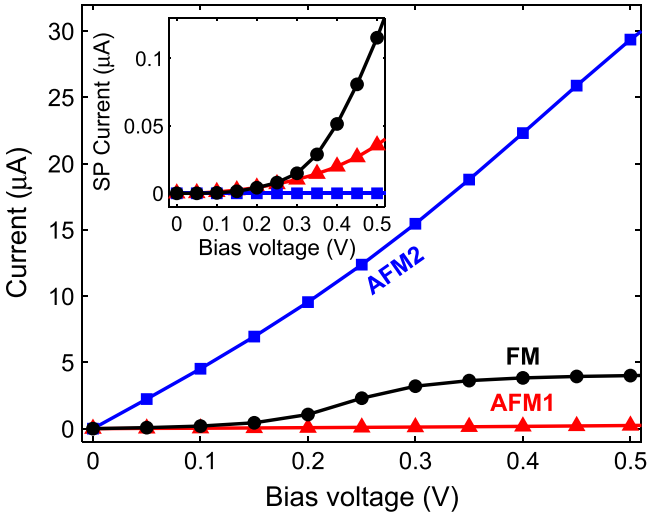

Figure 3. Current versus bias voltage calculated for three spin configurations at $T = 293$ K. Inset: spin polarized current.

The spin-polarized current is plotted in the inset of figure 3. It is noted that the current is at least two orders of magnitude smaller than the charge current. Surprisingly, when the device is in the AFM2 state, the spin-polarized current is seen to almost vanish even though there is a notable charge current through the nanojunction. In contrast, the AFM1 state is found to support a non-vanishing spin-polarized current in spite of the fact that the charge current is very small in this case. As for the FM state, we find that the corresponding spin-polarized current increases much more rapidly than the charge current after the bias voltage reaches the threshold of 0.2 V and does not show any sign of saturation.

We have shown that the *I/V* characteristics of the graphene nanojunction depends greatly on which spin configuration the device is operating in. In general, the system would choose to stay in a state of the lowest total energy. Figure 4 plots the total energies of three different spin configurations calculated as a function of the bias voltage. It is seen that AFM1 is the ground state where there is no bias voltage and remains the state of the lowest energy until the bias voltage is higher than about 0.4 V. It is also found that the total energies of both AFM1 and AFM2 exhibit very weak dependence on the applied bias voltage. In contrast, the FM state, being the highest one at zero bias, is seen to have a sensitive dependence of the total energy on the applied bias.

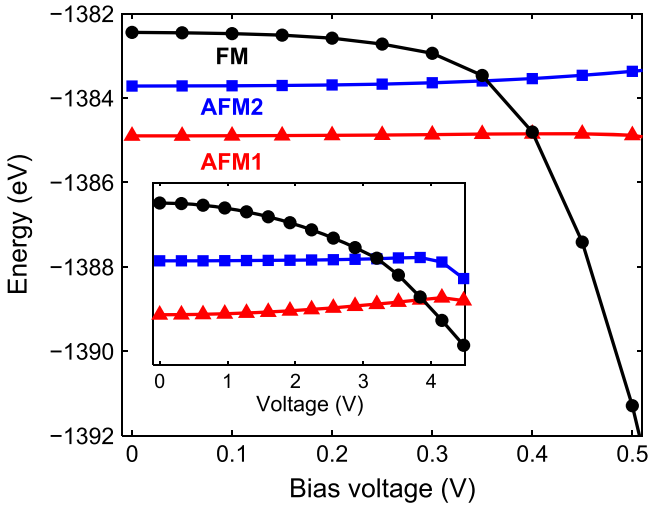

Figure 4. Total energy of the device for three stable spin configurations calculated as a function of the bias voltage. Inset: the energy calculated as a function of the electric field induced by the side gates.

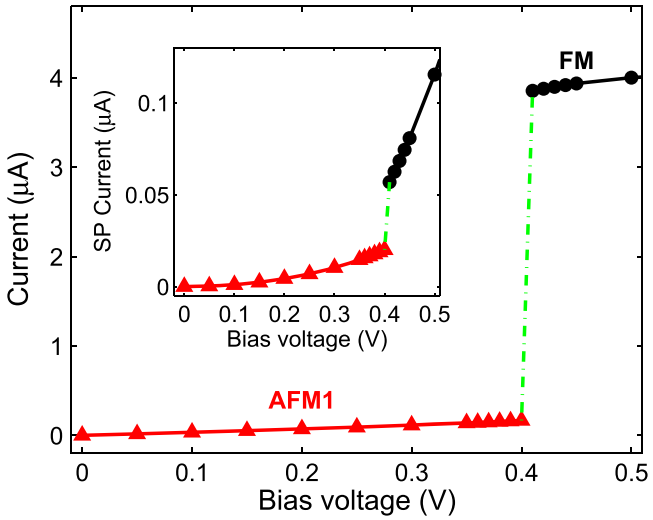

Figure 5. Current versus bias voltage for the device calculated at $T = 293$ K. Inset: spin polarized current.

Especially after the bias is beyond 0.3 V, the energy of FM is found to decrease rapidly and finally becomes the lowest one when the bias reaches about 0.4 V.

We hereby see that the ground state of the graphene nanojunction switches from an antiferromagnetic state (AFM1) to a ferromagnetic one (FM) as the bias voltage increases from zero to beyond 0.4 V. A similar magnetic transition may also be achieved by using a pair of side gates. Figure 4 plots the total energy of these three spin configurations as a function of the applied side-gate voltage in its inset. It is found that these states exhibit very similar dependence of the total energy on the applied voltage. The ground state of the system changes from AFM1 to FM when the side gate voltage reaches about 3.8 V which is almost one order of magnitude higher than what can be achieved with the bias voltage.

Taking this magnetic phase transition induced by the bias voltage into account, we can now obtain the final *I/V* curve of the device. Figure 5 shows the total current calculated as a function of the bias voltage. As expected, we see an abrupt change in the current as the ground state of the system changes from AFM1 to FM at around 0.4 V. It is noted, however, that a detailed description of the magnetic phase transition is beyond the scope of this work. Therefore, the result shown here represents only an idealized case. The spin-polarized current, as depicted in the inset, also exhibits an abrupt change, although much smaller, around the transition point.

The critical bias voltage, at which the magnetic transition occurs, is found to rely on both the Hubbard U and temperature. The dependence on the Hubbard U is rather sensitive as we find that the transition voltage decreases from 0.4 V at $U/t = 2.0$ to about 0.1 V when U/t is reduced to 1.8. This is mainly because the energy difference among the three spin configurations is determined largely by the Hubbard U. As for the temperature, the critical bias voltage is found to increase significantly as the temperature decreases. This can be understood by the fact that the high temperature actually increases the effective bias voltage.

4. Conclusions

In summary, we have demonstrated that magnetic phase transitions can be induced in a graphene nanojunction by an applied bias voltage without resorting to transverse gates. Combining the non-equilibrium Green's function with the Hubbard model, we have revealed that an increasing bias voltage would induce consecutive transitions among antiferromagnetic and ferromagnetic states. We have shown that the graphene nanojunction is turned off in the antiferromagnetic state with a low bias voltage and is switched on to the ferromagnetic state by a high bias voltage.

Acknowledgments

This work is supported by National Natural Science Foundation of China (Project No. 11474063) and National Basic Research Program of China (973 Program No. 2011CB925602).

References

[1] Yazyev O V 2010 *Rep. Prog. Phys.* **73** 056501
[2] Novoselov K S, Geim A K, Morozov S V, Jiang D, Zhang Y, Dubonos S V, Grigorieva I and Firsov A A 2004 *Science* **306** 666
[3] Wolf S A, Awschalom D D, Buhrman R A, Daughton J M, von Molnár S, Roukes M L, Chtchelkanova A Y and Treger D M 2001 *Science* **294** 1488
[4] Žutić I, Fabian J and das Sarma S 2004 *Rev. Mod. Phys.* **76** 323

[5] Seneor P, Dlubak B, Martin M B, Anane A, Jaffres H and Fert A 2012 *MRS Bull.* **37** 1245
[6] Pesin D and MacDonald A H 2012 *Nat. Mater.* **11** 409
[7] Roche S and Valenzuela S O 2014 *J. Phys. D: Appl. Phys* **47** 094011
[8] Nakada K, Fujita M, Dresselhaus G and Dresselhaus M S 1996 *Phys. Rev.* B **54** 24
[9] Guo X, Wang C and Zhou Y 2013 *Phys. Lett.* A **377** 993
[10] Güçlü A D and Hawrylak P 2013 *Phys. Rev.* B **87** 035425
[11] Szałowski K 2013 *J. Appl. Phys.* **114** 243908
[12] Zhou A, Sheng W and Xu S J 2013 *App. Phys. Lett.* **103** 133103
[13] Sheng W, Luo K and Zhou A 2014 *Phys. Rev.* B **90** 085406
[14] Szałowski K 2014 *Phys. Rev.* B **90** 085410
[15] Schwierz F 2010 *Nat. Nanotechnology* **5** 487
[16] Lu Y and Guo J 2010 *Appl. Phys. Lett.* **97** 073105
[17] Muñoz-Rojas F, Fernández-Rossier J and Palacios J J 2009 *Phys. Rev. Lett.* **102** 136810
[18] Ma Z and Sheng W 2011 *Appl. Phys. Lett.* **99** 083101
[19] Sheng W, Ning Z Y, Yang Z Q and Guo H 2010 *Nanotechnology* **21** 385201
[20] Ren H, Li Q X, Luo Y and Yang J 2009 *Appl. Phys. Lett.* **94** 173110
[21] Zhang Y T, Jiang H, Sun Q F and Xie X C 2010 *Phys. Rev.* B **81** 165404
[22] Son Y W, Cohen M L and Louie S G 2006 *Nature* **444** 347
[23] Guo J, Gunlycke D and White C T 2008 *Appl. Phys. Lett.* **92** 163109
[24] Jung J and MacDonald A H 2010 *Phys. Rev.* B **81** 195408
[25] Gunlycke D, Areshkin D A, Li J, Mintmire J W and White C T 2007 *Nano Lett.* **7** 3608
[26] Ozaki T, Nishio K and Kino H 2010 *Phys. Rev.* B **81** 035116
[27] Brandbyge M, Mozos J L, Ordejón P, Taylor J and Stokbro K 2002 *Phys. Rev.* B **65** 165401
[28] Luo Z, Kim S, Kawamoto N, Rappe A M and Johnson A T C 2011 *ACS Nano* **5** 9154
[29] Geng D, Wu B, Guo Y, Huang L, Xue Y, Chen J, Yu G, Jiang L, Hu W and Liu Y 2012 *Proc. Natl Acad. Sci* **109** 7992
[30] Kim W Y and Kim K S 2008 *J. Comput. Chem.* **29** 1073
[31] Li R, Zhang J, Hou S, Qian Z, Shen Z, Zhao X and Xue Z 2007 *Chem. Phys.* **336** 127
[32] Ozaki T 2007 *Phys. Rev.* B **75** 035123
[33] Datta S 2005 *Quantum Transport: Atom To Transistor* (Cambridge: Cambridge University Press)
[34] Ramo S, Whinnery J R and van Duzer T 1993 *Field and Wave in Communication Electronics* (New York: Wiley)
[35] Liang G C, Ghosh A W, Paulsson M and Datta S 2004 *Phys. Rev.* B **69** 115302
[36] Murrell J N and Harger A J 1972 *Semi-Empirical SCF MO Theory of Molecules* (London: Wiley)
[37] Luo K and Sheng W 2014 *J. Appl. Phys.* **115** 053705